Adaptive Refinement for *hp*-version Trefftz Discontinuous Galerkin Methods for the Homogeneous Helmholtz Problem

Scott Congreve

Fakultät für Mathematik, Universität Wien

Joint work with
Ilaria Perugia (Universität Wien)
Paul Houston (University of Nottingham)

University of Reading, September 14th 2018

Overview

1. Introduction
   - Helmholtz Equation
   - Continuous Galerkin FEM
   - Problems with FEM for Helmholtz
2. Trefftz DG (TDGFEM) for Helmholtz
   - Trefftz FEM Spaces
   - Plane Waves
   - Comparison to Polynomial DG
   - Formulation
3. Adaptive Refinement
   - Plane Wave Direction Refinement
   - A posteriori Error Estimates
   - *hp*-adaptive Refinement
   - Numerics

Section 1

Introduction

Let $\Omega \subset \mathbb{R}^d$, $d = 2, 3$ be a bounded polygonal/polyhedral domain. We seek $u : \Omega \mapsto \mathbb{C}$ such that

$$\begin{aligned} -\Delta u - k^2 u &= 0 && \text{in } \Omega, \\ u &= 0 && \text{on } \Gamma_D, \qquad \text{(sound-soft scattering)} \\ \nabla u \cdot \boldsymbol{n} + ik\vartheta u &= g_R && \text{on } \Gamma_R, \end{aligned}$$

where

$$k = \frac{\omega L}{c}$$

is the wavenumber (ω is the frequency of the wave, L is the measure of the domain, and c is the speed of sound in the material). Wavenumber is related to the wave length

$$\lambda = \frac{2\pi}{k}.$$

Multiplying by a test function and integrating by parts gives the weak formulation: Find $u \in H^1(\Omega)$ such that

$$\int_\Omega (\nabla u \cdot \nabla \bar{v} - k^2 u \bar{v})\, d\boldsymbol{x} + \int_{\Gamma_R} iku \cdot \boldsymbol{n} \bar{v}\, ds = \int_{\Gamma_R} g_R \cdot \boldsymbol{n} \bar{v}\, ds$$

for all $v \in H^1(\Omega)$.

Multiplying by a test function and integrating by parts gives the weak formulation: Find $u \in H^1(\Omega)$ such that

$$\int_\Omega (\nabla u \cdot \nabla \bar{v} - k^2 u \bar{v})\, d\boldsymbol{x} + \int_{\Gamma_R} iku \cdot \boldsymbol{n} \bar{v}\, ds = \int_{\Gamma_R} g_R \cdot \boldsymbol{n} \bar{v}\, ds$$

for all $v \in H^1(\Omega)$.

We want to search for a solution in a finite dimensional subspace of $H^1(\Omega)$. To that end we subdivide the domain Ω into a mesh $\mathcal{T}_h$ of non-overlapping elements K, where each element has a size h_K.

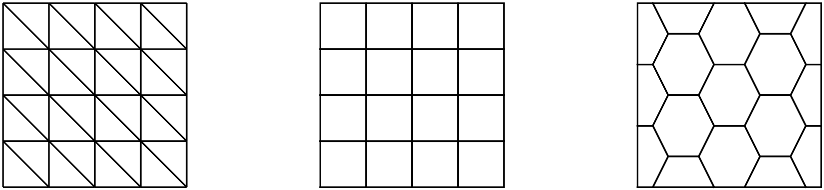

We can denote by $\mathcal{F}_h^I$, $\mathcal{F}_h^R$ and $\mathcal{F}_h^D$ all interior, Robin boundary, and Dirichlet boundary edges/faces, respectively.

FEM for Helmholtz

We can now define a subspace on this mesh:

$$V_q^{CG}(\mathcal{T}_h) \coloneqq \{v \in H^1(\Omega) : v|_K \in \mathcal{S}_q(K), K \in \mathcal{T}_h\} \subset H^1(\Omega),$$

then we can define the continuous Galerkin finite element method (CGFEM):

Find $u_h \in V_q^{CG}(\mathcal{T}_h)$ such that

$$\int_\Omega (\nabla u \cdot \nabla \bar{v} - k^2 u \bar{v})\, d\boldsymbol{x} + \int_{\Gamma_R} iku \cdot \boldsymbol{n} \bar{v}\, ds = \int_{\Gamma_R} g_R \cdot \boldsymbol{n} \bar{v}\, ds$$

for all $v_h \in V_q^{CG}(\mathcal{T}_h)$.

We can now define a subspace on this mesh:

$$V_q^{CG}(\mathcal{T}_h) := \{v \in H^1(\Omega) : v|_K \in \mathcal{S}_q(K), K \in \mathcal{T}_h\} \subset H^1(\Omega),$$

then we can define the continuous Galerkin finite element method (CGFEM):
Find $u_h \in V_q^{CG}(\mathcal{T}_h)$ such that

$$\int_\Omega (\nabla u \cdot \nabla \bar{v} - k^2 u \bar{v})\, d\boldsymbol{x} + \int_{\Gamma_R} iku \cdot \boldsymbol{n} \bar{v}\, ds = \int_{\Gamma_R} g_R \cdot \boldsymbol{n} \bar{v}\, ds$$

for all $v_h \in V_q^{CG}(\mathcal{T}_h)$.
We can also define a discontinuous Galerkin finite element method (DGFEM), where the space of functions is discontinuous over element boundaries:

$$V_q^{DG}(\mathcal{T}_h) := \{v \in L^2(\Omega) : v|_K \in \mathcal{S}_{q_K}(K), K \in \mathcal{T}_h\} \not\subset H^1(\Omega).$$

Here we integrate by parts elementwise and introduce fluxes on the edges/faces, Problems with FEM:

- Number of *degrees of freedom* required to obtain given accuracy increases with wave number k.
- h-version FEM affected by pollution effect [Babuška & Sauter, 2000]:

$$\|u - u_h\| \leq C(k) \inf_{v_h \in V_q^{CG}(\mathcal{T}_h)} \|u - v_h\|$$

$C(k)$ is an increasing function in k.

In order to minimise pollution it has been shown the following conditions should be met (for DGFEM):

$$p = \lceil ln(k) \rceil, \qquad \frac{kh}{p} \leq C.$$

[Sauter & Zech (2015)]

Section 2

Trefftz DG (TDGFEM) for Helmholtz

Polynomial DG Finite Element Spaces: DGFEM uses polynomial basis functions defined on a reference element $\widehat{K}$:

$$V_q^{DG}(\mathcal{T}_h) \coloneqq \{v \in L^2(\Omega) : v|_K \circ F_K \in \mathcal{S}_{q_K}(\widehat{K}), K \in \mathcal{T}_h\}.$$

Trefftz FEM Spaces

Polynomial DG Finite Element Spaces: DGFEM uses polynomial basis functions defined on a reference element $\widehat{K}$:

$$V_q^{DG}(\mathcal{T}_h) := \{v \in L^2(\Omega) : v|_K \circ F_K \in \mathcal{S}_{q_K}(\widehat{K}), K \in \mathcal{T}_h\}.$$

Trefftz Finite Element Space: Use basis functions defined element-wise based on functions in the kernel of the Helmholtz operator.
First define the local Trefftz spaces

$$T(K) := \{v|_K : -\Delta u - k^2 u = 0\}$$

and let

$$T(\mathcal{T}_h) := \{v \in L^2(\Omega) : v|_K \in T(K), K \in \mathcal{T}_h\}.$$

Polynomial DG Finite Element Spaces: DGFEM uses polynomial basis functions defined on a reference element $\widehat{K}$:

$$V_q^{DG}(\mathcal{T}_h) := \{v \in L^2(\Omega) : v|_K \circ F_K \in \mathcal{S}_{q_K}(\widehat{K}), K \in \mathcal{T}_h\}.$$

Trefftz Finite Element Space: Use basis functions defined element-wise based on functions in the kernel of the Helmholtz operator.
First define the local Trefftz spaces

$$T(K) := \{v|_K : -\Delta u - k^2 u = 0\}$$

and let

$$T(\mathcal{T}_h) := \{v \in L^2(\Omega) : v|_K \in T(K), K \in \mathcal{T}_h\}.$$

We let $V_p(K) \subset T(K)$ be a finite dimensional local space; then, the Trefftz FE Space is given by

$$V_p(\mathcal{T}_h) := \{v \in T(\mathcal{T}_h) : v_K \in V_p(K), K \in \mathcal{T}_h\}.$$

For Helmholtz we can use the following basis functions:

Plane Waves: $\boldsymbol{x} \mapsto \mathrm{e}^{ik\boldsymbol{d}\cdot\boldsymbol{x}}$, where $\boldsymbol{d}$ is a direction vector.

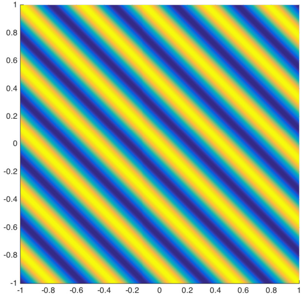

For Helmholtz we can use the following basis functions:

Plane Waves: $\boldsymbol{x} \mapsto \mathrm{e}^{ik\boldsymbol{d}\cdot\boldsymbol{x}}$, where $\boldsymbol{d}$ is a direction vector.

Circular/Spherical Waves $\boldsymbol{x} \mapsto \mathcal{J}_\ell(k|\boldsymbol{x}|)\mathrm{e}^{i\ell\theta}$ (in 2D), where θ is the angle of $\boldsymbol{x}$ in polar coordinates, $\ell \in \mathbb{Z}$, and $\mathcal{J}_\ell$ is the Bessel function of the first kind of order ℓ.

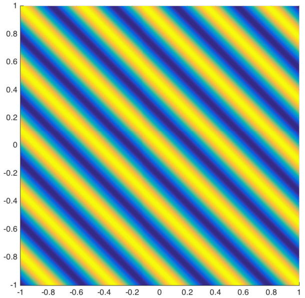

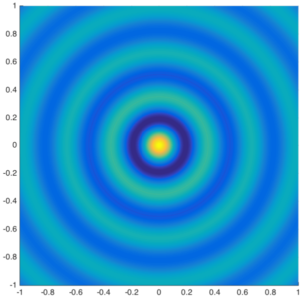

Plane Waves

$$V_p(K) = \left\{ v : v(\boldsymbol{x}) = \sum_{\ell=1}^{p_K} \alpha_\ell \mathrm{e}^{ik\boldsymbol{d}_\ell\cdot(\boldsymbol{x}-\boldsymbol{x}_K)}, \alpha_\ell \in \mathbb{C} \right\}$$

where p_K is the number of *degrees of freedom* for the element K, $\boldsymbol{d}_\ell$, $\ell = 1, \ldots, p_K$ are p_K (roughly) evenly spaced unit direction vectors, and $\boldsymbol{x}_K$ is the centre of the element.

Plane Waves

$$V_p(K) = \left\{ v : v(\boldsymbol{x}) = \sum_{\ell=1}^{p_K} \alpha_\ell \mathrm{e}^{ik\boldsymbol{d}_\ell\cdot(\boldsymbol{x}-\boldsymbol{x}_K)}, \alpha_\ell \in \mathbb{C} \right\}$$

where p_K is the number of *degrees of freedom* for the element K, $\boldsymbol{d}_\ell$, $\ell = 1, \ldots, p_K$ are p_K (roughly) evenly spaced unit direction vectors, and $\boldsymbol{x}_K$ is the centre of the element.

Number of directions can be selected to give the same accuracy as a high-order polynomial DG method of order q with less degrees of freedom.

Basis Functions	2D	3D
DG ($\mathcal{P}_q$)	$(q+1)(q+2)/2$	$(q+1)(q+2)(q+3)/6$
DG ($\mathcal{Q}_q$)	$(q+1)^2$	$(q+1)^3$
Trefftz DG	$2q+1$	$(q+1)^2$

Number of Degrees of Freedom

$$V_p(K) = \left\{ v : v(\boldsymbol{x}) = \sum_{\ell=1}^{p_K} \alpha_\ell \mathrm{e}^{ik\boldsymbol{d}_\ell \cdot (\boldsymbol{x} - \boldsymbol{x}_K)}, \alpha_\ell \in \mathbb{C} \right\}$$

where p_K is the number of *degrees of freedom* for the element K, $\boldsymbol{d}_\ell$, $\ell = 1, \ldots, p_K$ are p_K (roughly) evenly spaced unit direction vectors, and $\boldsymbol{x}_K$ is the centre of the element.

Number of directions can be selected to give the same accuracy as a high-order polynomial DG method of order q with less degrees of freedom.

Basis Functions	2D	3D
DG ($\mathcal{P}_q$)	$(q+1)(q+2)/2$	$(q+1)(q+2)(q+3)/6$
DG ($\mathcal{Q}_q$)	$(q+1)^2$	$(q+1)^3$
Trefftz DG	$2q+1$	$(q+1)^2$

Number of Degrees of Freedom

Direction Vectors ($q = 3$):

2D

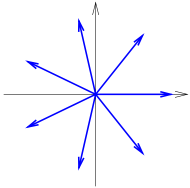

3D

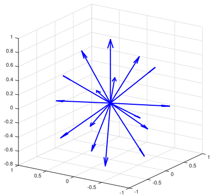

[Sloan & Womersley, 2004]

TDG/DG FEM Comparison

Consider the smooth (analytic) solution (for Acoustic Wave Propagation)

$$u(r,\theta) = \mathcal{J}_1(kr)\cos(\theta)$$

for $k = 20$ on the domain $\Omega = (0,1) \times (-1/2, 1/2)$.

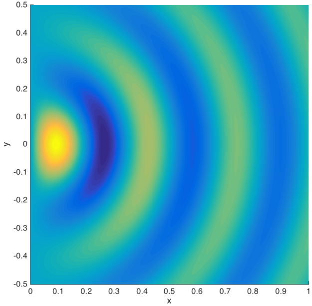

Analytical Solution
(Real Part)

Consider the smooth (analytic) solution (for Acoustic Wave Propagation)

$$u(r,\theta) = \mathcal{J}_1(kr)\cos(\theta)$$

for $k = 20$ on the domain $\Omega = (0,1) \times (-1/2, 1/2)$.
We solve using both a DGFEM (solid line) and Trefftz DGFEM (dashed).

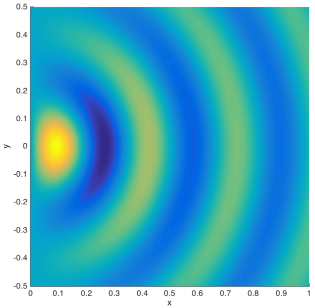

Analytical Solution (Real Part)

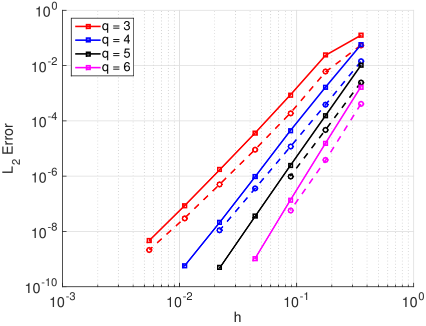

$\|u - u_{hp}\|_{L^2(\Omega)}$ vs. h (h-refinement)

TDG/DG FEM Comparison

Consider the smooth (analytic) solution (for Acoustic Wave Propagation)

$$u(r,\theta) = \mathcal{J}_1(kr)\cos(\theta)$$

for $k = 20$ on the domain $\Omega = (0,1) \times (-1/2, 1/2)$.
We solve using both a DGFEM (solid line) and Trefftz DGFEM (dashed).

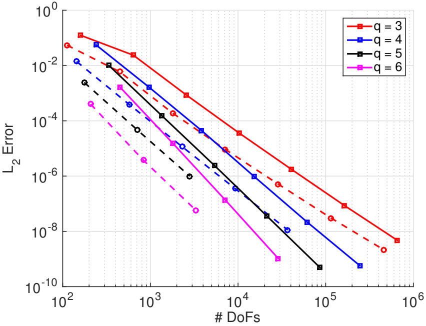

$\|u - u_{hp}\|_{L^2(\Omega)}$ vs. Degrees of Freedom
(h-refinement)

TDG/DG FEM Comparison

Consider the smooth (analytic) solution (for Acoustic Wave Propagation)

$$u(r,\theta) = \mathcal{J}_1(kr)\cos(\theta)$$

for $k = 20$ on the domain $\Omega = (0,1) \times (-1/2, 1/2)$.
We solve using both a DGFEM (solid line) and Trefftz DGFEM (dashed).

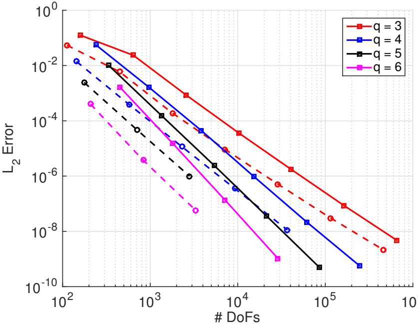

$\|u - u_{hp}\|_{L^2(\Omega)}$ vs. Degrees of Freedom (h-refinement)

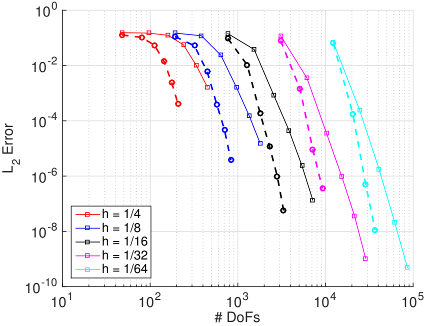

$\|u - u_{hp}\|_{L^2(\Omega)}$ vs. Degrees of Freedom (p-refinement)

Given a mesh $\mathcal{T}_h$ on Ω we derive the TDGFEM as follows.

Given a mesh $\mathcal{T}_h$ on Ω we derive the TDGFEM as follows.

- Multiply by test functions and integrate by parts, element-wise, twice (ultra weak formulation):

$$\int_K (-\Delta u - k^2 u)\, \bar{v} \quad d\boldsymbol{x} \qquad = 0$$

TDGFEM for Helmholtz

Given a mesh $\mathcal{T}_h$ on Ω we derive the TDGFEM as follows.

- Multiply by test functions and integrate by parts, element-wise, twice (ultra weak formulation):

$$\int_K (\nabla u \cdot \nabla \bar{v} - k^2 u \bar{v}) \, d\boldsymbol{x} \qquad - \int_{\partial K} \nabla u \cdot \boldsymbol{n}_K \bar{v} \, ds = 0$$

Given a mesh $\mathcal{T}_h$ on Ω we derive the TDGFEM as follows.

- Multiply by test functions and integrate by parts, element-wise, twice (ultra weak formulation):

$$\int_K u(-\Delta \bar{v} - k^2 \bar{v}) \; d\boldsymbol{x} + \int_{\partial K} u \nabla \bar{v} \cdot \boldsymbol{n}_K \, ds - \int_{\partial K} \nabla u \cdot \boldsymbol{n}_K \bar{v} \, ds = 0$$

Given a mesh $\mathcal{T}_h$ on Ω we derive the TDGFEM as follows.

- Multiply by test functions and integrate by parts, element-wise, twice (ultra weak formulation):

$$\int_K u(-\Delta \bar{v} - k^2 \bar{v}) \quad d\boldsymbol{x} + \int_{\partial K} u \nabla \bar{v} \cdot \boldsymbol{n}_K \, ds - \int_{\partial K} \nabla u \cdot \boldsymbol{n}_K \bar{v} \, ds = 0$$

Given a mesh $\mathcal{T}_h$ on Ω we derive the TDGFEM as follows.

- Multiply by test functions and integrate by parts, element-wise, twice (ultra weak formulation):

$$\int_K u(-\Delta \bar{v} - k^2 \bar{v}) \quad d\boldsymbol{x} + \int_{\partial K} u \nabla \bar{v} \cdot \boldsymbol{n}_K \, ds - \int_{\partial K} \nabla u \cdot \boldsymbol{n}_K \bar{v} \, ds = 0$$

- Replace continuous functions by discrete approximations ($u_{hp}, v_{hp} \in V_p(\mathcal{T}_h)$) and traces by numerical fluxes

$$u \rightarrow \widehat{u}_{hp}, \qquad \nabla u \rightarrow ik\widehat{\boldsymbol{\sigma}}_{hp}.$$

Given a mesh $\mathcal{T}_h$ on Ω we derive the TDGFEM as follows.

- Multiply by test functions and integrate by parts, element-wise, twice (ultra weak formulation):

$$\int_K u(-\Delta \bar{v} - k^2 \bar{v}) \;\; d\boldsymbol{x} + \int_{\partial K} u \nabla \bar{v} \cdot \boldsymbol{n}_K \, ds - \int_{\partial K} \nabla u \cdot \boldsymbol{n}_K \bar{v} \, ds = 0$$

- Replace continuous functions by discrete approximations ($u_{hp}, v_{hp} \in V_p(\mathcal{T}_h)$) and traces by numerical fluxes

$$u \to \widehat{u}_{hp}, \qquad \nabla u \to ik\widehat{\boldsymbol{\sigma}}_{hp}.$$

- $v \in V_p(\mathcal{T}_h) \subset T(\mathcal{T}_h) \quad \Longrightarrow \quad -\Delta \bar{v} - k^2 \bar{v} = 0 \text{ in } K.$

TDGFEM for Helmholtz

Given a mesh $\mathcal{T}_h$ on Ω we derive the TDGFEM as follows.

- Multiply by test functions and integrate by parts, element-wise, twice (ultra weak formulation):

$$\int_K u(-\Delta \bar{v} - k^2 \bar{v}) \;\; d\boldsymbol{x} + \int_{\partial K} u \nabla \bar{v} \cdot \boldsymbol{n}_K \, ds - \int_{\partial K} \nabla u \cdot \boldsymbol{n}_K \bar{v} \, ds = 0$$

- Replace continuous functions by discrete approximations ($u_{hp}, v_{hp} \in V_p(\mathcal{T}_h)$) and traces by numerical fluxes

$$u \to \widehat{u}_{hp}, \qquad \nabla u \to ik\widehat{\boldsymbol{\sigma}}_{hp}.$$

- $v \in V_p(\mathcal{T}_h) \subset T(\mathcal{T}_h) \quad \Longrightarrow \quad -\Delta \bar{v} - k^2 \bar{v} = 0$ in K.

$$\int_{\partial K} \widehat{u}_{hp} \nabla \bar{v}_{hp} \cdot \boldsymbol{n}_K \, ds - \int_{\partial K} ik\widehat{\boldsymbol{\sigma}}_{hp} \cdot \boldsymbol{n}_K \bar{v}_{hp} \, ds = 0, \qquad \text{for all } K \in \mathcal{T}_h.$$

$$\{\!\{v\}\!\} = \frac{v^+ + v^-}{2}, \quad [\![v]\!] = v^+\boldsymbol{n}^+ + v^-\boldsymbol{n}^-, \qquad \forall \text{ scalar-valued functions } v.$$

$$\{\!\{\boldsymbol{\tau}\}\!\} = \frac{\boldsymbol{\tau}^+ + \boldsymbol{\tau}^-}{2}, \quad [\![\boldsymbol{\tau}]\!] = \boldsymbol{\tau}^+ \cdot \boldsymbol{n}^+ + \boldsymbol{\tau}^- \cdot \boldsymbol{n}^-, \quad \forall \text{ vector-valued functions } \boldsymbol{\tau}.$$

$$\{\!\{v\}\!\} = \frac{v^+ + v^-}{2}, \quad [\![v]\!] = v^+\boldsymbol{n}^+ + v^-\boldsymbol{n}^-, \qquad \forall \text{ scalar-valued functions } v.$$

$$\{\!\{\boldsymbol{\tau}\}\!\} = \frac{\boldsymbol{\tau}^+ + \boldsymbol{\tau}^-}{2}, \quad [\![\boldsymbol{\tau}]\!] = \boldsymbol{\tau}^+\cdot\boldsymbol{n}^+ + \boldsymbol{\tau}^-\cdot\boldsymbol{n}^-, \quad \forall \text{ vector-valued functions } \boldsymbol{\tau}.$$

Numerical Fluxes

$$ik\widehat{\boldsymbol{\sigma}}_{hp} = \begin{cases} \{\!\{\nabla_h u_{hp}\}\!\} - \alpha ik[\![u_{hp}]\!] & \text{on interior faces,} \\ \nabla_h u_{hp} - (1-\delta)\left(\nabla_h u_{hp} + ik\vartheta u_{hp}\boldsymbol{n} - g_R\boldsymbol{n}\right) & \text{on faces on } \Gamma_R, \\ \nabla_h u_{hp} - \alpha ik u_{hp}\boldsymbol{n} & \text{on faces on } \Gamma_D, \end{cases}$$

$$\widehat{u}_{hp} = \begin{cases} \{\!\{u_{hp}\}\!\} - \beta(ik)^{-1}[\![\nabla_h u_{hp}]\!] & \text{on interior faces,} \\ u_{hp} - \delta\left((ik\vartheta)^{-1}\nabla_h u_{hp}\cdot\boldsymbol{n} + u_{hp} - (ik\vartheta)^{-1}g_R\right) & \text{on faces on } \Gamma_R, \\ 0 & \text{on faces on } \Gamma_D, \end{cases}$$

with flux parameters α, β, $0 < \delta \leq 1/2$.

universität wien

Trefftz Discontinuous Galerkin FEM for Helmholtz

Find $u_{hp} \in V_p(\mathcal{T}_h)$ such that,

$$\mathcal{A}_h(u_{hp}, v_{hp}) = \ell_h(v_{hp}),$$

for all $v_{hp} \in V_p(\mathcal{T}_h)$, where

$$\begin{aligned}
\mathcal{A}_h(u, v) = & \int_{\mathcal{F}_h^I} \{\!\{u\}\!\} [\![\nabla_h \bar{v}]\!] \, ds - \int_{\mathcal{F}_h^I} \beta (ik)^{-1} [\![\nabla_h u]\!][\![\nabla_h \bar{v}]\!] \, ds \\
& - \int_{\mathcal{F}_h^I \cup \mathcal{F}_h^D} \{\!\{\nabla_h u\}\!\} \cdot [\![\bar{v}]\!] \, ds + \int_{\mathcal{F}_h^I \cup \mathcal{F}_h^D} \alpha ik [\![u]\!] \cdot [\![\bar{v}]\!] \, ds \\
& + \int_{\mathcal{F}_h^R} (1 - \delta) u \nabla_h \bar{v} \cdot \boldsymbol{n} \, ds - \int_{\mathcal{F}_h^R} \delta (ik\vartheta)^{-1} (\nabla_h u \cdot \boldsymbol{n})(\nabla_h \bar{v} \cdot \boldsymbol{n}) \, ds \\
& - \int_{\mathcal{F}_h^R} \delta \nabla_h u \cdot \boldsymbol{n} \bar{v} \, ds + \int_{\mathcal{F}_h^R} (1 - \delta) ik\vartheta u \bar{v} \, ds, \\
\ell_h(v) = & - \int_{\mathcal{F}_h^R} \delta (ik\vartheta)^{-1} g_R \nabla_h \bar{v} \cdot \boldsymbol{n} \, ds + \int_{\mathcal{F}_h^R} (1 - \delta) g_R \bar{v} \, ds.
\end{aligned}$$

Flux Parameters

Penalty Type	α	β	δ
DG-type Gittelson, Hiptmair & Perugia, 2009	$\mathtt{a}q_K^2/kh_K$	$\mathtt{b}kh_K/q_K$	$\mathtt{d}kh_K/q_K$
Constant Hiptmair, Moiola & Perugia, 2011	$\mathtt{a}$	$\mathtt{b}$	$\mathtt{d}$
UWVF Cessenat & Després, 1998	$1/2$	$1/2$	$1/2$
Non-Uniform Mesh Hiptmair, Moiola & Perugia, 2014	$\mathtt{a}h_{\max}/h_K$	$\mathtt{b}h_{\max}/h_K$	$\mathtt{d}h_{\max}/h_K$

Section 3

Adaptive Refinement

Plane Wave Direction Refinement

Selecting plane wave directions which align with the wave direction of the analytical solution can reduce the error.
Several existing approaches exist for selecting pane wave directions:

- Ray-tracing — requires a source term. [Betcke & Phillips, 2012]
- Approximate

$$\frac{\nabla e(\boldsymbol{x}_0)}{ike(\boldsymbol{x}_0)},$$

  where e is the error. [Gittelson, 2008 (Master's Thesis)]
- Adding an extra unknown (the optimal angle of rotation) to the basis functions. [Amara, Chaudhry, Diaz, Djellouli & Fiedler, 2014]

Plane Wave Direction Refinement

Selecting plane wave directions which align with the wave direction of the analytical solution can reduce the error.

Several existing approaches exist for selecting pane wave directions:

- Ray-tracing — requires a source term. [Betcke & Phillips, 2012]
- Approximate
$$\frac{\nabla e(\boldsymbol{x}_0)}{ike(\boldsymbol{x}_0)},$$
where e is the error. [Gittelson, 2008 (Master's Thesis)]
- Adding an extra unknown (the optimal angle of rotation) to the basis functions. [Amara, Chaudhry, Diaz, Djellouli & Fiedler, 2014]

We propose using the Hessian of the numerical solution, based on work on anisotropic meshes for standard FE [Formaggia & Perotto, 2001, 2003].

Plane Wave Direction Refinement

Plane Wave Refinement Algorithm (2D)

Let $(\lambda_1, \boldsymbol{v}_1), (\lambda_2, \boldsymbol{v}_2)$ be the eigenpairs of $\mathbf{H}(\mathrm{Re}(u_h(\boldsymbol{x}_K)))$, and $(\mu_1, \boldsymbol{w}_1), (\mu_2, \boldsymbol{w}_2)$ the eigenpairs of $\mathbf{H}(\mathrm{Im}(u_h(\boldsymbol{x}_K)))$ s.t. $|\lambda_1| \geq |\lambda_2|$, $|\mu_1| \geq |\mu_2|$; then, for constant $C > 1$, we can select the first plane wave direction as follows:

$\|\lambda_1\| \geq C\|\lambda_2\|$	$\|\mu_1\| \geq C\|\mu_2\|$	$\|\lambda_1\| \geq C\|\mu_1\|$	$\|\mu_1\| \geq C\|\lambda_1\|$	First PW
✓	✓	✓	✗	$\boldsymbol{v}_1$
✓	✓	✗	✓	$\boldsymbol{w}_1$
✓	✓	✗	✗	$\frac{(\boldsymbol{v}_1+\boldsymbol{w}_1)}{\|\boldsymbol{v}_1+\boldsymbol{w}_1\|}$
✓	✗	✓	✗	$\boldsymbol{v}_1$
✓	✗	✗	–	–
✗	✓	✗	✓	$\boldsymbol{w}_1$
✗	✓	–	✗	–
✗	✗	–	–	–

[C., Houston, Perugia (2018)]

If $\boldsymbol{v}$ is the eigenvector, then the direction of propagation could be either $\boldsymbol{v}$ or $-\boldsymbol{v}$ (unknown orientation). Consider the impedance on the boundary of a ball (radius δ around $\boldsymbol{x}_K$) and compare to the plane wave $u(\boldsymbol{x}) = \mathrm{e}^{ik\boldsymbol{d}\cdot(\boldsymbol{x}-\boldsymbol{x}_K)}$ for the cases when $\boldsymbol{d} = \boldsymbol{v}$ and $\boldsymbol{d} = -\boldsymbol{v}$.

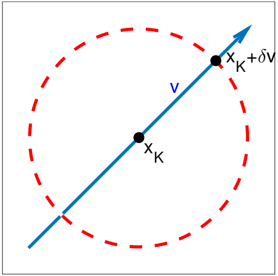

Plane Wave Direction Refinement

If $\boldsymbol{v}$ is the eigenvector, then the direction of propagation could be either $\boldsymbol{v}$ or $-\boldsymbol{v}$ (unknown orientation). Consider the impedance on the boundary of a ball (radius δ around $\boldsymbol{x}_K$) and compare to the plane wave $u(\boldsymbol{x}) = \mathrm{e}^{ik\boldsymbol{d}\cdot(\boldsymbol{x}-\boldsymbol{x}_K)}$ for the cases when $\boldsymbol{d} = \boldsymbol{v}$ and $\boldsymbol{d} = -\boldsymbol{v}$.

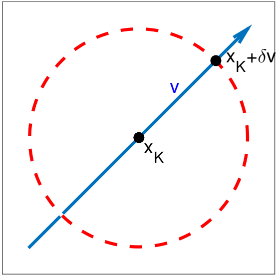

Evaluating at $\boldsymbol{x}_K + \delta\boldsymbol{v}$ we note that the normal is $\boldsymbol{v}$, so we can calculate

$$\frac{\nabla u_h(\boldsymbol{x}_K + \delta\boldsymbol{v}) \cdot \boldsymbol{v} + iku_h(\boldsymbol{x}_K + \delta\boldsymbol{v})}{iku_h(\boldsymbol{x}_K + \delta\boldsymbol{v})}.$$

If $\boldsymbol{v}$ is the eigenvector, then the direction of propagation could be either $\boldsymbol{v}$ or $-\boldsymbol{v}$ (unknown orientation). Consider the impedance on the boundary of a ball (radius δ around $\boldsymbol{x}_K$) and compare to the plane wave $u(\boldsymbol{x}) = \mathrm{e}^{ik\boldsymbol{d}\cdot(\boldsymbol{x}-\boldsymbol{x}_K)}$ for the cases when $\boldsymbol{d} = \boldsymbol{v}$ and $\boldsymbol{d} = -\boldsymbol{v}$.

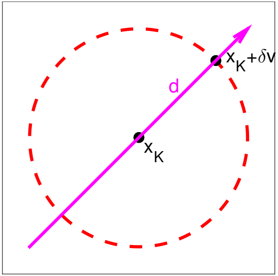

Evaluating at $\boldsymbol{x}_K + \delta\boldsymbol{v}$ we note that the normal is $\boldsymbol{v}$, so we can calculate

$$\frac{\nabla u_h(\boldsymbol{x}_K + \delta\boldsymbol{v}) \cdot \boldsymbol{v} + iku_h(\boldsymbol{x}_K + \delta\boldsymbol{v})}{iku_h(\boldsymbol{x}_K + \delta\boldsymbol{v})}.$$

We can compare this to the impedance for u:

$$\frac{\nabla u(\boldsymbol{x}_K + \delta\boldsymbol{v}) \cdot \boldsymbol{v}}{iku(\boldsymbol{x}_K + \delta\boldsymbol{v})} + 1 = \begin{cases} 2, & \text{if } \boldsymbol{d} = \boldsymbol{v}, \\ \end{cases}$$

If $\boldsymbol{v}$ is the eigenvector, then the direction of propagation could be either $\boldsymbol{v}$ or $-\boldsymbol{v}$ (unknown orientation). Consider the impedance on the boundary of a ball (radius δ around $\boldsymbol{x}_K$) and compare to the plane wave $u(\boldsymbol{x}) = \mathrm{e}^{ik\boldsymbol{d}\cdot(\boldsymbol{x}-\boldsymbol{x}_K)}$ for the cases when $\boldsymbol{d} = \boldsymbol{v}$ and $\boldsymbol{d} = -\boldsymbol{v}$.

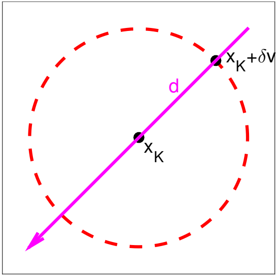

Evaluating at $\boldsymbol{x}_K + \delta\boldsymbol{v}$ we note that the normal is $\boldsymbol{v}$, so we can calculate

$$\frac{\nabla u_h(\boldsymbol{x}_K + \delta\boldsymbol{v}) \cdot \boldsymbol{v} + iku_h(\boldsymbol{x}_K + \delta\boldsymbol{v})}{iku_h(\boldsymbol{x}_K + \delta\boldsymbol{v})}.$$

We can compare this to the impedance for u:

$$\frac{\nabla u(\boldsymbol{x}_K + \delta\boldsymbol{v}) \cdot \boldsymbol{v}}{iku(\boldsymbol{x}_K + \delta\boldsymbol{v})} + 1 = \begin{cases} 2, & \text{if } \boldsymbol{d} = \boldsymbol{v}, \\ 0, & \text{if } \boldsymbol{d} = -\boldsymbol{v}. \end{cases}$$

To test the direction refinement, we consider the solution

$$u(x, y) = \mathcal{H}_0^{(1)}(k\sqrt{(x + 0.25)^2 + y^2}),$$

with $k = 20$, on the domain $\Omega = (0, 1)^2$.

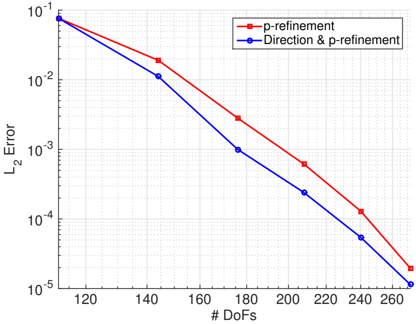

$\|u - u_{hp}\|_{L^2(\Omega)}$ vs. DoF

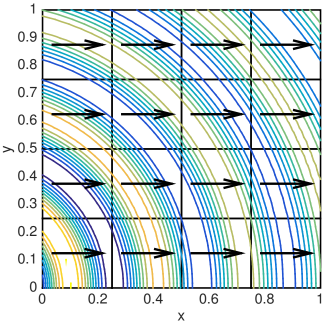

First PW Direction ($p = 3$)

To test the direction refinement, we consider the solution

$$u(x,y) = \mathcal{H}_0^{(1)}(k\sqrt{(x+0.25)^2 + y^2}),$$

with $k = 20$, on the domain $\Omega = (0,1)^2$.

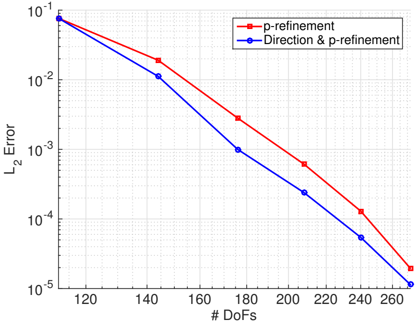

$\|u - u_{hp}\|_{L^2(\Omega)}$ vs. *DoF*

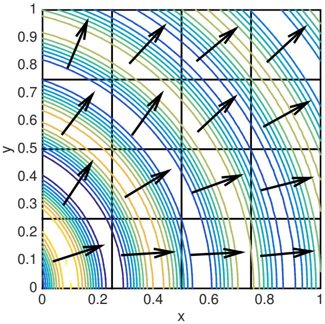

First PW Direction ($p = 4$)

To test the direction refinement, we consider the solution

$$u(x,y) = \mathcal{H}_0^{(1)}(k\sqrt{(x+0.25)^2+y^2}),$$

with $k = 20$, on the domain $\Omega = (0,1)^2$.

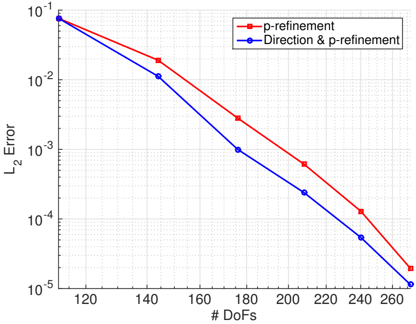

$\|u - u_{hp}\|_{L^2(\Omega)}$ vs. *DoF*

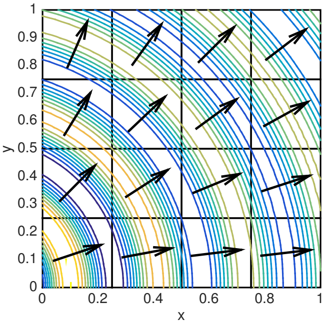

First PW Direction ($p = 5$)

To test the direction refinement, we consider the solution

$$u(x, y) = \mathcal{H}_0^{(1)}(k\sqrt{(x + 0.25)^2 + y^2}),$$

with $k = 20$, on the domain $\Omega = (0, 1)^2$.

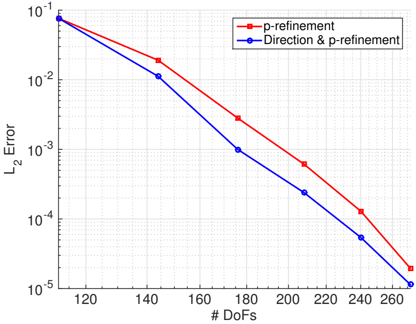

$\|u - u_{hp}\|_{L^2(\Omega)}$ vs. DoF

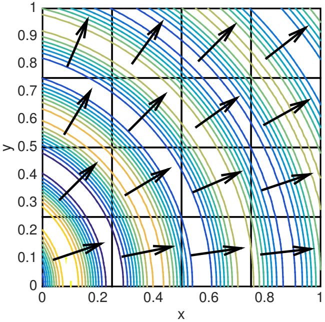

First PW Direction ($p = 6$)

To test the direction refinement, we consider the solution

$$u(x,y) = \mathcal{H}_0^{(1)}(k\sqrt{(x+0.25)^2+y^2}),$$

with $k = 20$, on the domain $\Omega = (0,1)^2$.

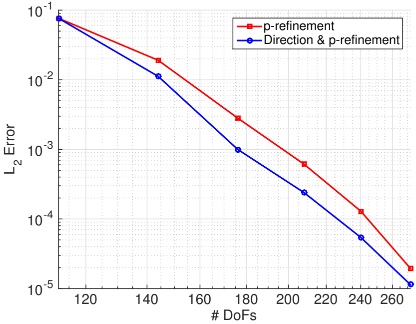

$\|u - u_{hp}\|_{L^2(\Omega)}$ vs. *DoF*

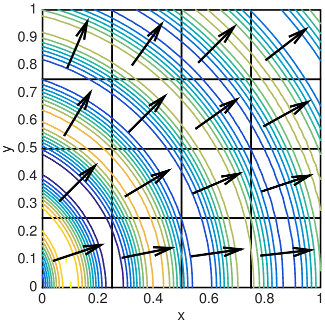

First PW Direction ($p = 7$)

To test the direction refinement, we consider the solution

$$u(x,y) = \mathcal{H}_0^{(1)}(k\sqrt{(x+0.25)^2+y^2}),$$

with $k = 20$, on the domain $\Omega = (0,1)^2$.

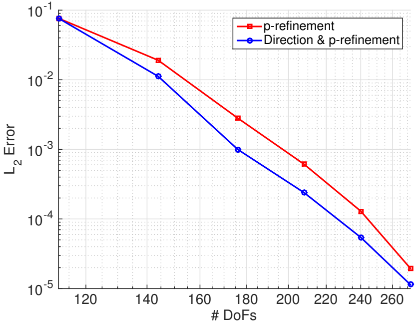

$\|u - u_{hp}\|_{L^2(\Omega)}$ vs. *DoF*

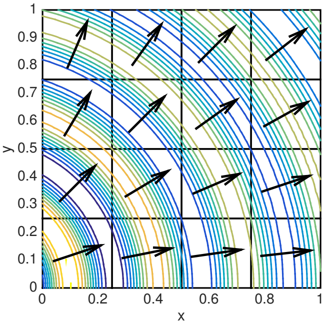

First PW Direction ($p = 8$)

An *a posteriori* error bounds exists for the *h*-version of the method in $\mathbb{R}_2$.

A posteriori Error Bound — *h*-version Only

For the TDGFEM, with the constant flux parameters, the following error bound holds:

$$\|u - u_h\|^2_{L^2(\Omega)} \leq C(k, d_\Omega)\Bigg\{ \left\|\alpha^{1/2} h_F^s [\![u_h]\!]\right\|^2_{L^2(\mathcal{F}_h^I \cup \mathcal{F}_h^D)} + \frac{1}{k^2}\|\beta^{\frac{1}{2}} h_F^s [\![\nabla u_h]\!]\|^2_{L^2(\mathcal{F}_h^I)} + \frac{1}{k^2}\left\|\delta^{1/2} h_F^s \left(g_R - \nabla u_h \cdot \boldsymbol{n}_F + ik\vartheta u_h\right)\right\|^2_{L^2(\mathcal{F}_h^R)} \Bigg\}$$

where s depends on the regularity of the solution to the adjoint problem ($z \in H^{3/2+s}(\Omega)$).

[Kapita, Monk & Warburton, 2015]

A posteriori Error Bound — *hp*-version

We propose the following potential *a posteriori* error bound with constants derived numerical to ensure the bound is efficient:

$$\|u - u_{hp}\|^2_{L^2(\Omega)} \leq C \Big\{ k \Big\| \alpha^{1/2} h_F^{1/2} q_F^{-1/2} [\![u_{hp}]\!] \Big\|^2_{L^2(\mathcal{F}_h^I \cup \mathcal{F}_h^D)} + \|\beta^{\frac{1}{2}} h_F^{3/2} q_F^{-3/2} [\![\nabla u_{hp}]\!] \|^2_{L^2(\mathcal{F}_h^I)} + \Big\| \delta^{1/2} h_F^{3/2} q_F^{-3/2} \left(g_R - \nabla u_{hp} \cdot \boldsymbol{n}_F + iku_{hp} \right) \Big\|^2_{L^2(\mathcal{F}_h^R)} \Big\}$$

for smooth solution of the adjoint.

[C., Houston, Perugia (2018)]

Modified *hp*-refinement Strategy [Melenk & Wohlmuth, 2001]

Let $\mathcal{T}_{h,0}$ be the initial mesh, $\mathcal{T}_{h,i}$ the mesh after i refinements, $\eta_{K,i}$ the error indicator for $K \in \mathcal{T}_{h,i}$, and $\eta_{K,i}^{\text{pred}}$ the predicted error for $K \in \mathcal{T}_{h,i}$.

for $K \in \mathcal{T}_{h,i}$ **do**
  if K is marked for refinement **then**
    if $\eta_{K,i}^2 > (\eta_{K,i}^{\text{pred}})^2$ **then**
      h-refinement: Subdivide K into N sons $K_s, s \in 0, \ldots, N$
      $(\eta_{K_s,i+1}^{\text{pred}})^2 \leftarrow \frac{1}{N}\gamma_h \left(\frac{1}{2}\right)^{2q_K} \eta_{K,i}^2,\ i \leq s \leq N$
    else
      p-refinement: $q_K \leftarrow q_K + 1$
      $(\eta_{K,i+1}^{\text{pred}})^2 \leftarrow \gamma_p \eta_{K,i}^2$
    end if
  else
    $(\eta_{K,i+1}^{\text{pred}})^2 \leftarrow \gamma_n (\eta_{K,i}^{\text{pred}})^2$
  end if
end for

Consider the smooth (analytic) solution (for Acoustic Wave Propagation)

$$u(x,y) = \mathcal{H}_0^{(1)}\left(k\sqrt{(x+1/4)^2+y^2}\right),$$

on the domain $\Omega = (0,1)^2$ with suitable Robin BCs.
Consider h- and hp-refinement for $k = 20$.

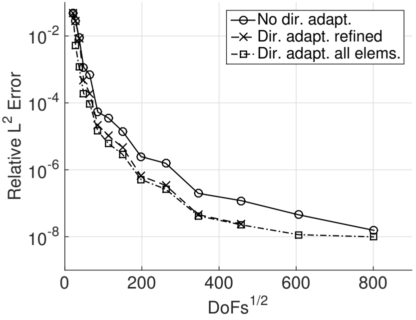

L^2-Error & Error Bound

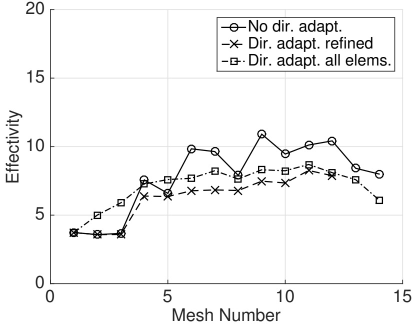

Effectivity

Consider the smooth (analytic) solution (for Acoustic Wave Propagation)

$$u(x,y) = \mathcal{H}_0^{(1)}\left(k\sqrt{(x+1/4)^2+y^2}\right),$$

on the domain $\Omega = (0,1)^2$ with suitable Robin BCs.
Consider h- and hp-refinement for $k = 20$.

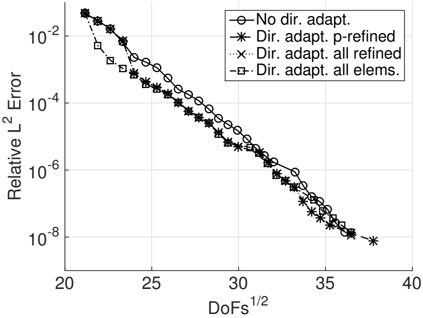

L^2-Error & Error Bound

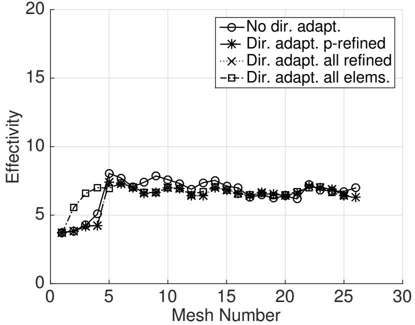

Effectivity

Consider the smooth (analytic) solution (for Acoustic Wave Propagation)

$$u(x, y) = \mathcal{H}_0^{(1)}(k\sqrt{(x + 1/4)^2 + y^2}),$$

on the domain $\Omega = (0, 1)^2$ with suitable Robin BCs.
Consider h- and hp-refinement for $k = 20$.

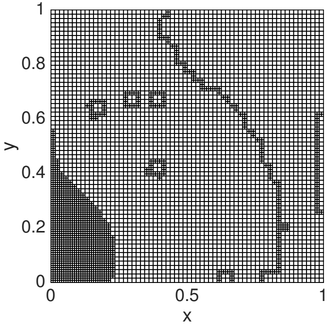

Mesh after 8 h-refinements

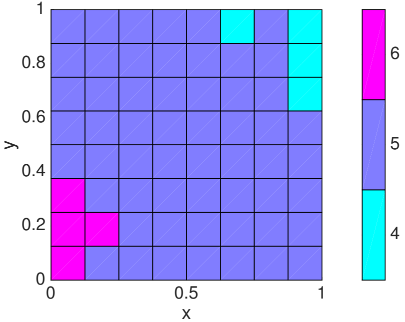

Mesh after 8 hp-refinements

Consider the smooth (analytic) solution (for Acoustic Wave Propagation)

$$u(x,y) = \mathcal{H}_0^{(1)}(k\sqrt{(x+1/4)^2+y^2}),$$

on the domain $\Omega = (0,1)^2$ with suitable Robin BCs.
Consider h- and hp-refinement for $k = 50$.

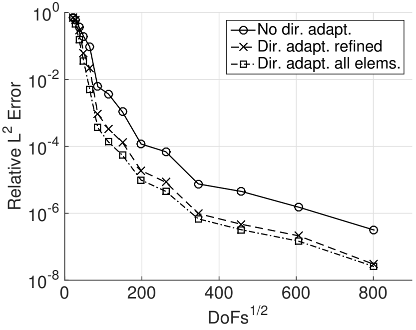

L^2-Error & Error Bound

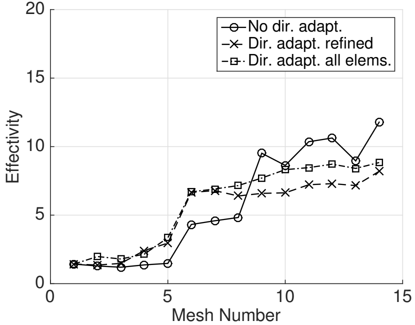

Effectivity

Consider the smooth (analytic) solution (for Acoustic Wave Propagation)

$$u(x, y) = \mathcal{H}_0^{(1)}(k\sqrt{(x + 1/4)^2 + y^2}),$$

on the domain $\Omega = (0, 1)^2$ with suitable Robin BCs.
Consider *h*- and *hp*-refinement for $k = 50$.

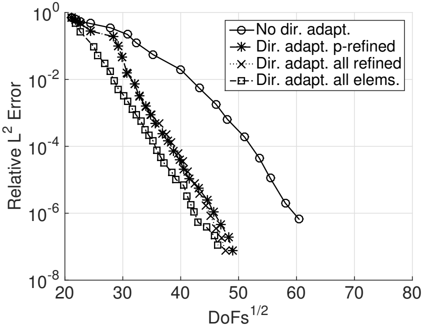

L^2-Error & Error Bound

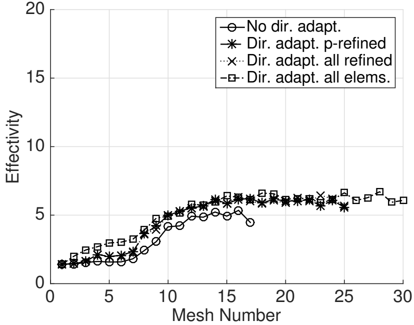

Effectivity

Consider the smooth (analytic) solution (for Acoustic Wave Propagation)

$$u(x,y) = \mathcal{H}_0^{(1)}(k\sqrt{(x+1/4)^2+y^2}),$$

on the domain $\Omega = (0,1)^2$ with suitable Robin BCs.
Consider h- and hp-refinement for $k = 50$.

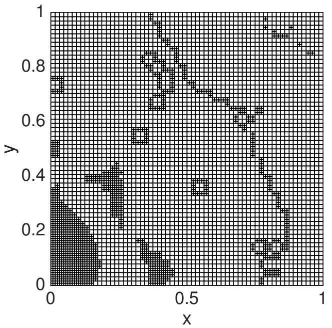

Mesh after 8 h-refinements

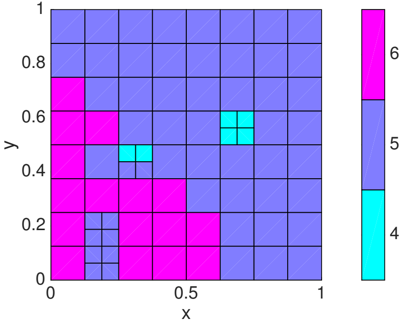

Mesh after 8 hp-refinements

Consider the 3D smooth (analytic) solution (for Acoustic Wave Propagation)

$$u(\boldsymbol{x}) = \mathrm{e}^{ik\boldsymbol{d}\cdot\boldsymbol{x}},$$

on the domain $\Omega = (0,1)^3$, where $\boldsymbol{d}_i = 1/\sqrt{3}$ for $i = 1,2,3$, with suitable Robin BCs.

Consider h- and hp-refinement for $k = 20$.

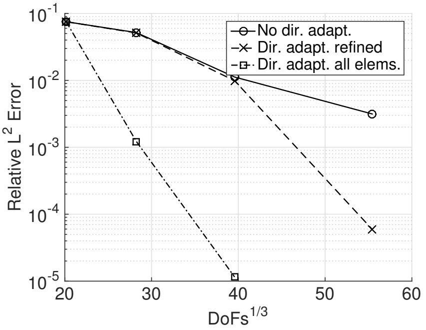

L^2-Error & Error Bound

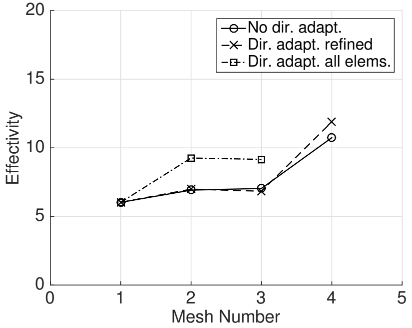

Effectivity

Adaptive Refinement

Consider the 3D smooth (analytic) solution (for Acoustic Wave Propagation)

$$u(\boldsymbol{x}) = \mathrm{e}^{ik\boldsymbol{d}\cdot\boldsymbol{x}},$$

on the domain $\Omega = (0,1)^3$, where $\boldsymbol{d}_i = 1/\sqrt{3}$ for $i = 1,2,3$, with suitable Robin BCs.

Consider h- and hp-refinement for $k = 20$.

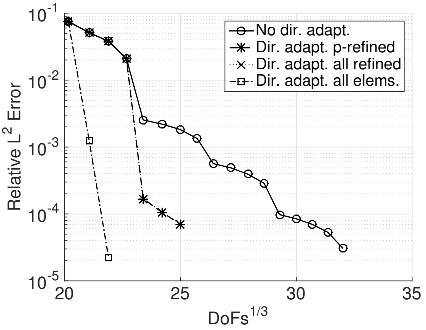

L^2-Error & Error Bound

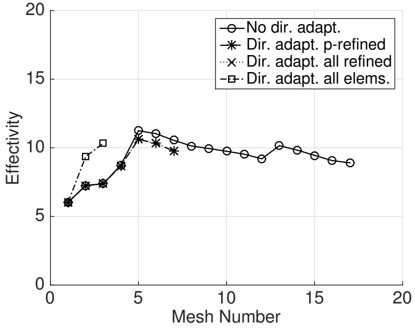

Effectivity

Consider the 3D smooth (analytic) solution (for Acoustic Wave Propagation)

$$u(\boldsymbol{x}) = \mathrm{e}^{ik\boldsymbol{d}\cdot\boldsymbol{x}},$$

on the domain $\Omega = (0,1)^3$, where $\boldsymbol{d}_i = 1/\sqrt{3}$ for $i = 1, 2, 3$, with suitable Robin BCs.

Consider h- and hp-refinement for $k = 50$.

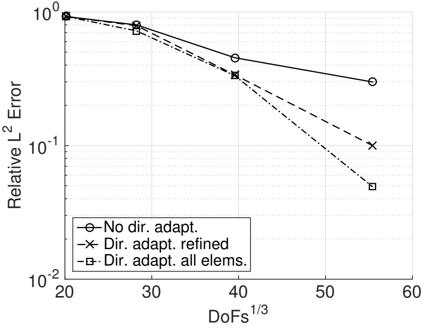

L^2-Error & Error Bound

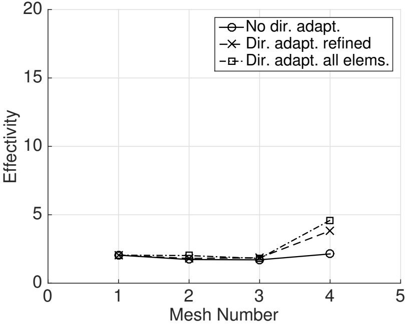

Effectivity

Consider the 3D smooth (analytic) solution (for Acoustic Wave Propagation)

$$u(\boldsymbol{x}) = \mathrm{e}^{ik\boldsymbol{d}\cdot\boldsymbol{x}},$$

on the domain $\Omega = (0,1)^3$, where $\boldsymbol{d}_i = 1/\sqrt{3}$ for $i = 1, 2, 3$, with suitable Robin BCs.

Consider h- and hp-refinement for $k = 50$.

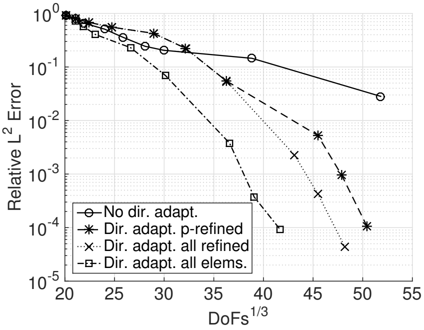

L^2-Error & Error Bound

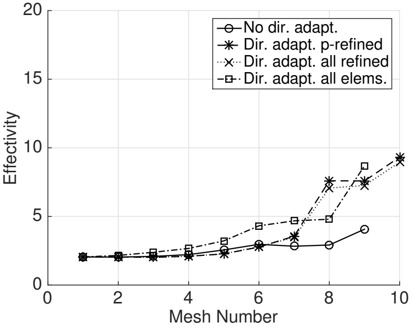

Effectivity

Consider the non-smooth solution (for Acoustic Wave Propagation)

$$u(r,\theta) = \mathcal{J}_{2/3}(kr)\sin(2\theta/3),$$

on the domain L-shaped domain $\Omega = (-1,1)^2 \setminus (0,1) \times (-1,1)$, with suitable Robin BCs.

Consider h- and hp-refinement for $k = 20$.

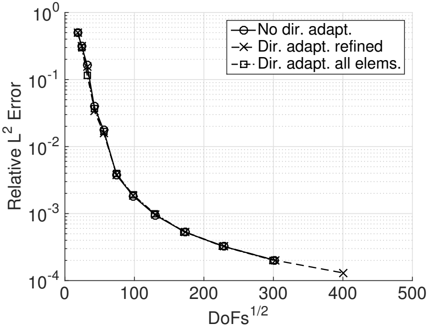

L^2-Error & Error Bound

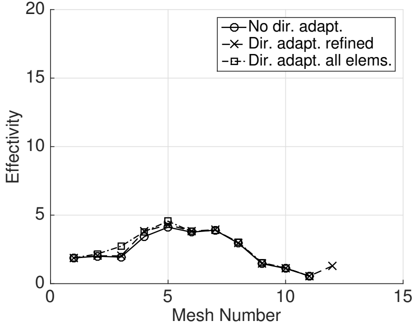

Effectivity

Consider the non-smooth solution (for Acoustic Wave Propagation)

$$u(r,\theta) = \mathcal{J}_{2/3}(kr)\sin({}^{2\theta}/_{3}),$$

on the domain L-shaped domain $\Omega = (-1,1)^2 \setminus (0,1) \times (-1,1)$, with suitable Robin BCs.

Consider h- and hp-refinement for $k = 20$.

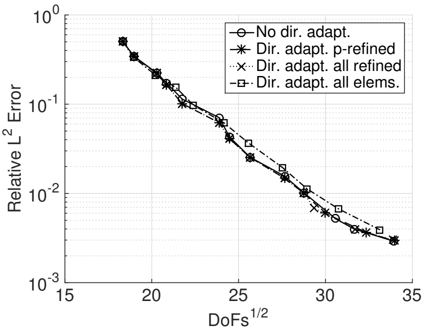

L^2-Error & Error Bound

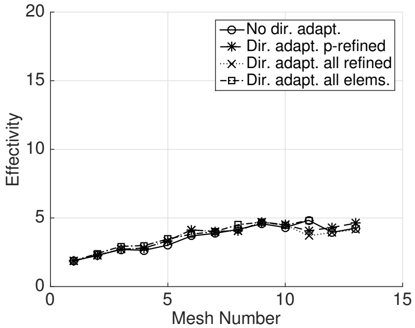

Effectivity

Consider the non-smooth solution (for Acoustic Wave Propagation)

$$u(r,\theta) = \mathcal{J}_{2/3}(kr)\sin({}^{2\theta}/_{3}),$$

on the domain L-shaped domain $\Omega = (-1,1)^2 \setminus (0,1) \times (-1,1)$, with suitable Robin BCs.
Consider h- and hp-refinement for $k = 20$.

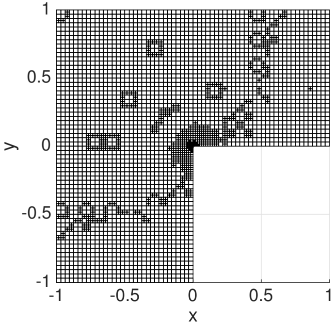

Mesh after 8 h-refinements

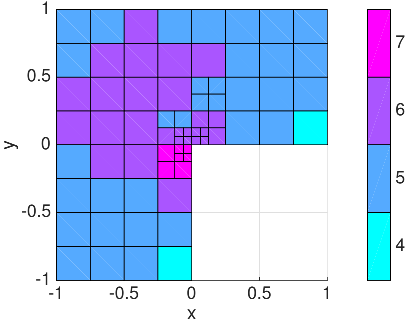

Mesh after 8 hp-refinements

Adaptive Refinement

Consider the non-smooth solution (for Acoustic Wave Propagation)

$$u(r,\theta) = \mathcal{J}_{2/3}(kr)\sin(2\theta/3),$$

on the domain L-shaped domain $\Omega = (-1,1)^2 \setminus (0,1) \times (-1,1)$, with suitable Robin BCs.

Consider *h*- and *hp*-refinement for $k = 50$.

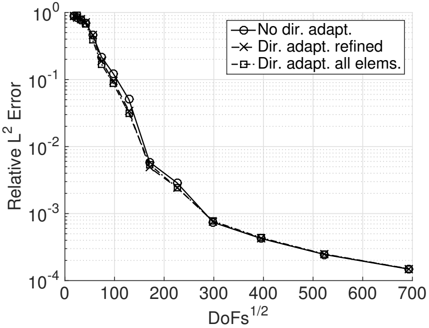

L^2-Error & Error Bound

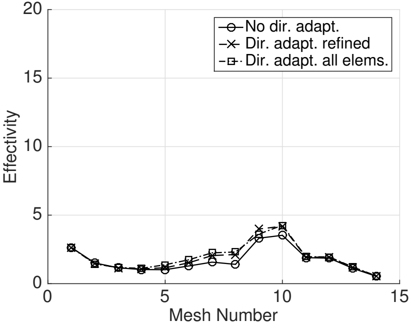

Effectivity

Adaptive Refinement

Consider the non-smooth solution (for Acoustic Wave Propagation)

$$u(r,\theta) = \mathcal{J}_{2/3}(kr)\sin(2\theta/3),$$

on the domain L-shaped domain $\Omega = (-1,1)^2 \setminus (0,1) \times (-1,1)$, with suitable Robin BCs.

Consider h- and hp-refinement for $k = 50$.

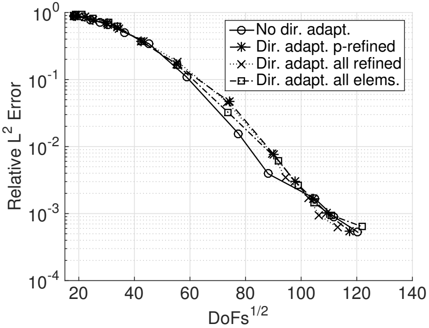

L^2-Error & Error Bound

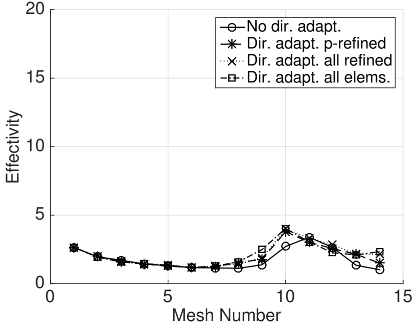

Effectivity

Consider the non-smooth solution (for Acoustic Wave Propagation)

$$u(r,\theta) = \mathcal{J}_{2/3}(kr)\sin(2\theta/3),$$

on the domain L-shaped domain $\Omega = (-1,1)^2 \setminus (0,1) \times (-1,1)$, with suitable Robin BCs.

Consider h- and hp-refinement for $k = 50$.

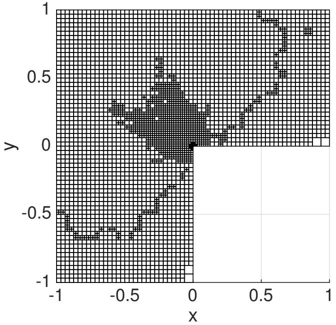

Mesh after 8 h-refinements

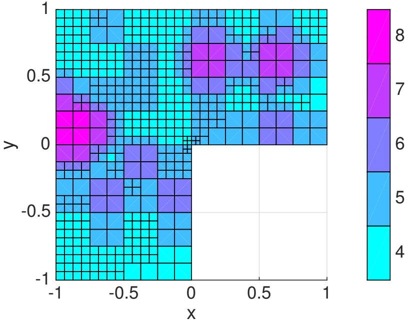

Mesh after 8 hp-refinements

We now consider a wavenumber k given by the piecewise constant function

$$k(x,y) = \begin{cases} k_1 := \omega n_1 & \text{if } y \le 0, \\ k_2 := \omega n_2 & \text{if } y > 0, \end{cases}$$

where, we $\omega = 11$, $n_1 = 2$, and $n_2 = 1$, with appropriate inhomogeneous Dirichlet boundary condition, such that , for a constant $0 \le \theta_i \le \pi/2$,

$$u(x,y) = \begin{cases} T\mathrm{e}^{i(K_1 x + K_2 y)} & \text{if } y > 0, \\ \mathrm{e}^{ik_1(x\cos(\theta_i) + y\sin(\theta_i))} + R\mathrm{e}^{ik_1(x\cos(\theta_i) - y\sin(\theta_i))} & \text{if } y < 0, \end{cases}$$

where $K_1 = k_1 \cos(\theta_i)$, $K_2 = \sqrt{k_2^2 - k_1^2 \cos^2(\theta_i)}$,

$$R = -\frac{K_2 - k_1 \sin(\theta_i)}{K_2 + k_1 \sin(\theta_i)},$$

and $T = 1 + R$.

There exists a critical angle θ_{crit}, such that when $\theta_i > \theta_{crit}$ the wave is refracted, while $\theta_i < \theta_{crit}$ results in internal reflection.

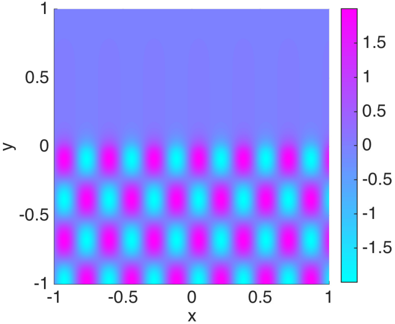

$\theta_i = 29^\circ$ — Analytical Soln.

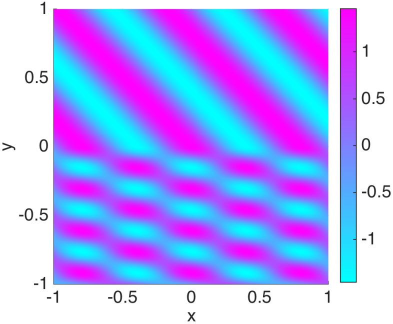

$\theta_i = 69^\circ$ — Analytical Soln.

There exists a critical angle θ_{crit}, such that when $\theta_i > \theta_{crit}$ the wave is refracted, while $\theta_i < \theta_{crit}$ results in internal reflection.

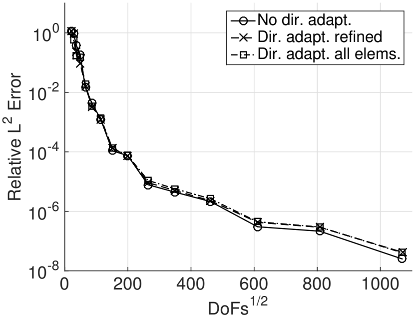

$\theta_i = 29^\circ$ — L^2-Error & Error Bound (h)

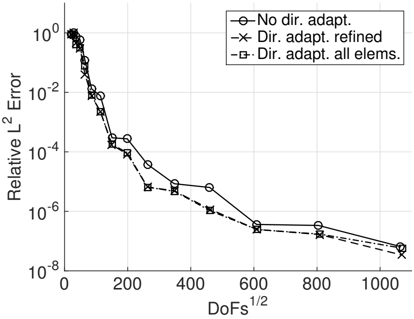

$\theta_i = 69^\circ$ — L^2-Error & Error Bound (h)

There exists a critical angle θ_{crit}, such that when $\theta_i > \theta_{crit}$ the wave is refracted, while $\theta_i < \theta_{crit}$ results in internal reflection.

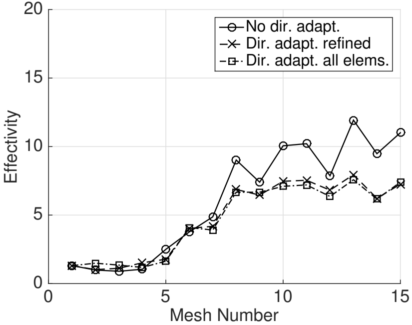

$\theta_i = 29^\circ$ — Effectivity (h)

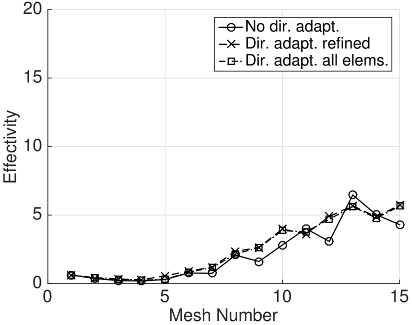

$\theta_i = 69^\circ$ — Effectivity (h)

There exists a critical angle θ_{crit}, such that when $\theta_i > \theta_{crit}$ the wave is refracted, while $\theta_i < \theta_{crit}$ results in internal reflection.

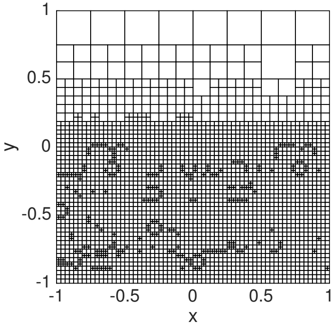

$\theta_i = 29^\circ$ — Mesh after 7 *hp*-refinements

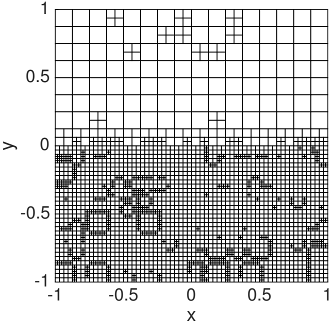

$\theta_i = 69^\circ$ — Mesh after 7 *h*-refinements

Adaptive Refinement

There exists a critical angle θ_{crit}, such that when $\theta_i > \theta_{crit}$ the wave is refracted, while $\theta_i < \theta_{crit}$ results in internal reflection.

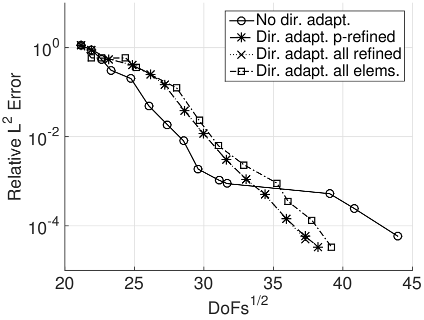

$\theta_i = 29^\circ$ — L^2-Error & Error Bound (hp)

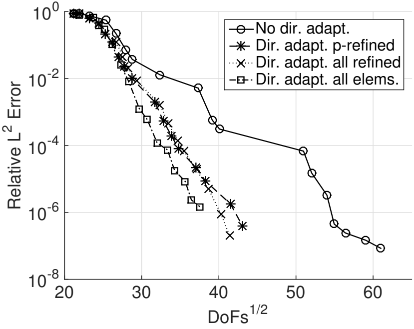

$\theta_i = 69^\circ$ — L^2-Error & Error Bound (hp)

There exists a critical angle θ_{crit}, such that when $\theta_i > \theta_{crit}$ the wave is refracted, while $\theta_i < \theta_{crit}$ results in internal reflection.

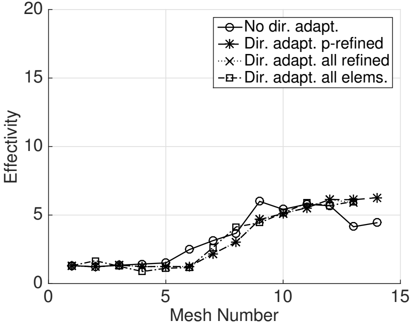

$\theta_i = 29^\circ$ — Effectivity (hp)

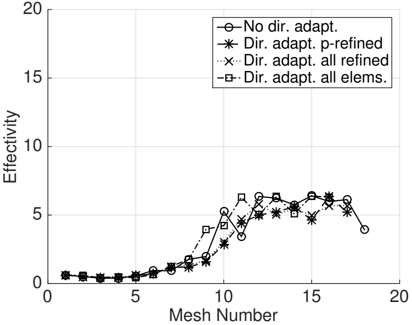

$\theta_i = 69^\circ$ — Effectivity (hp)

There exists a critical angle θ_{crit}, such that when $\theta_i > \theta_{crit}$ the wave is refracted, while $\theta_i < \theta_{crit}$ results in internal reflection.

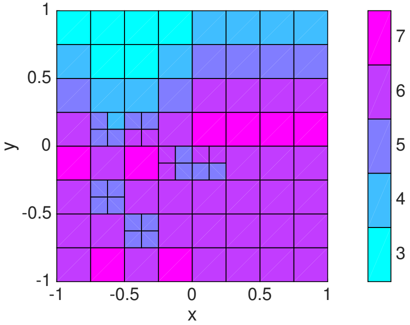

$\theta_i = 29°$ — Mesh after 7 *hp*-refinements

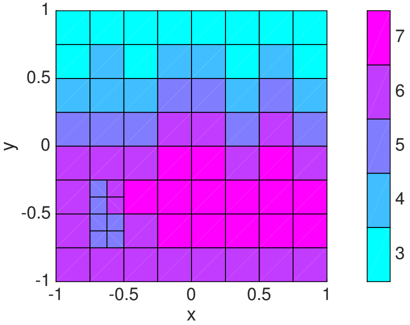

$\theta_i = 69°$ — Mesh after 7 *hp*-refinements

Consider a scattering problem around an obstacle (kite). We impose homogeneous Dirichlet boundary conditions on the obstacle, and Robin boundary condition

$$g_R(\boldsymbol{x}) = \mathrm{e}^{ik\boldsymbol{d}\cdot\boldsymbol{x}}$$

with $k = 20$ and $\boldsymbol{d} = -(\cos(6\pi/13), \sin(6\pi/13))^\top$.

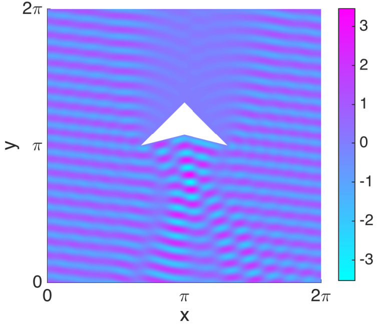

Consider a scattering problem around an obstacle (kite). We impose homogeneous Dirichlet boundary conditions on the obstacle, and Robin boundary condition

$$g_R(\boldsymbol{x}) = \mathrm{e}^{ik\boldsymbol{d}\cdot\boldsymbol{x}}$$

with $k = 20$ and $\boldsymbol{d} = -(\cos(6\pi/13), \sin(6\pi/13))^\top$.

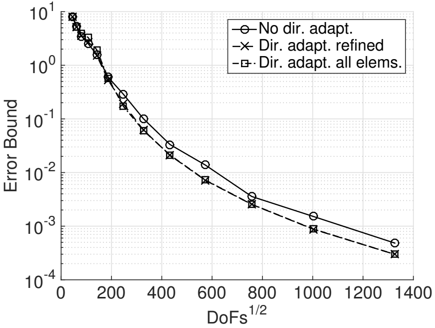

Error Bound (h)

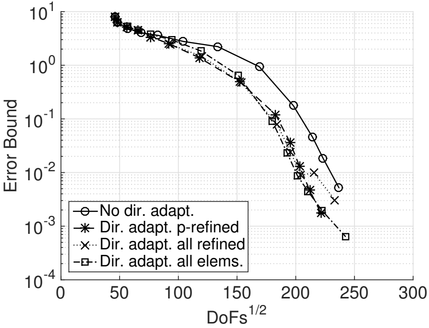

Error Bound (hp)

Consider a scattering problem around an obstacle (kite). We impose homogeneous Dirichlet boundary conditions on the obstacle, and Robin boundary condition

$$g_R(\boldsymbol{x}) = \mathrm{e}^{ik\boldsymbol{d}\cdot\boldsymbol{x}}$$

with $k = 20$ and $\boldsymbol{d} = -(\cos(6\pi/13), \sin(6\pi/13))^\top$.

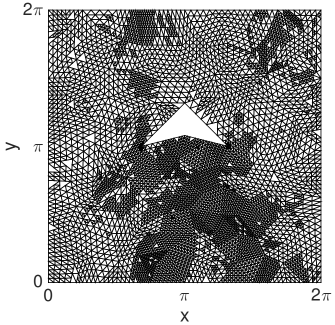

Mesh after 9 *h*-refinements

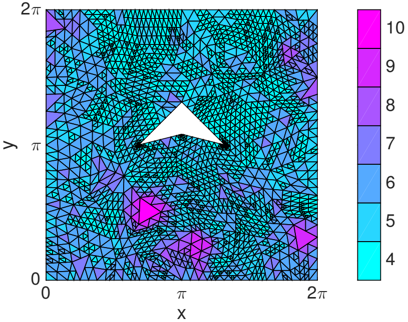

Mesh after 9 *hp*-refinements

Consider a scattering problem around an obstacle (kite). We impose homogeneous Dirichlet boundary conditions on the obstacle, and Robin boundary condition

$$g_R(\boldsymbol{x}) = \mathrm{e}^{ik\boldsymbol{d}\cdot\boldsymbol{x}}$$

with $k = 20$ and $\boldsymbol{d} = -(\cos(6\pi/13), \sin(6\pi/13))^\top$.

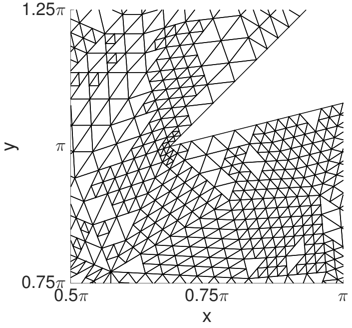

Mesh after 9 *h*-refinements

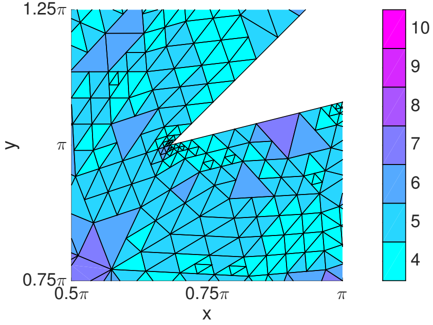

Mesh after 9 *hp*-refinements

Conclusion

Summary:

- With plane wave basis functions it is possible to refine the wave directions.
- *hp*-adaptive refinement results in exponential convergence.
- Combining plane wave direction adaptivity with *hp*-adaptive refinement often leads to reduced error compared to standard refinement.

Future Aims:

- Develop robust *hp*-version *a posteriori* error bounds..
- Use the eigenvalues/eigenvectors to develop anisotropic *p*-refinement (unevenly spaced plane waves).